Fracture Mechanics of Concrete and Concrete Structures -
Assessment, Durability, Monitoring and Retrofitting of Concrete Structures- B. H. Oh, et al. (eds)

Investigations on the mechanism of concrete cover cracking due to reinforcement corrosion

E. Bohner, H.S. Müller & S. Bröhl
Institute of Concrete Structures and Building Materials, Karlsruhe Institute of Technology, Germany

ABSTRACT: The corrosion of the reinforcement usually results in cracking and spalling of the concrete cover. Both types of damage define important limit states of durability and structural stability of reinforced concrete structures. The mechanism of fracture and the magnitude of stresses causing cracking and spalling of the concrete are still unknown and can only be simulated incompletely so far. Thus, a realistic and quantitative description as well as a reliable prediction of the time development of the damage process due to reinforcement corrosion is not possible. Therefore, the aim of the presented work is the development of a comprehensive analytical prediction model, which describes the time dependent damage process of cracking and spalling under realistic conditions. Since the accuracy of such an analytical model depends primarily on the quality of the implemented constitutive models, a main target of the work is to determine the mechanical properties of the corrosion products by applying novel experiments and inverse analyses. By means of numerical investigations applying fracture mechanical concepts and being supplemented with experimental results, first a numerical model of the cracking and damage process was developed. This modelling approach, involving sophisticated material laws, allows for the detailed analysis of the stresses, strains and the crack formation within the concrete cover as well as for a realistic prediction of the time development of cover cracking caused by the corrosion of the reinforcement. Based on parameter studies of several specimens, which are subjected to different corrosive conditions, the comprehensive analytical prediction model for the time dependent damage process can be derived. This model will enable the prediction of damage development under conditions of practical relevance and serves as a part of a full probabilistic design approach for durability of reinforced concrete structures.

1 INTRODUCTION

In the last decades numerous research studies had been carried out on reinforcement corrosion in concrete. However, research on the corrosion effect on structural serviceability remains still unsatisfactory. So far, most of the analytical investigations in this field were accomplished by the use of finite element analyses (e.g. Bhargava et al. 2005, Toongoenthong & Maekawa 2005) based on models, which describe the process of concrete cover cracking only in a qualitative way. Aspects of fracture mechanics and time dependent effects as shrinkage and creep of the concrete were mostly neglected. A major deficiency in previous investigations is the ignorance of a constitutive model for rust. Thus, it is impossible to evaluate realistic time intervals for the appearance of corrosion damage.

The experimental investigations, which are currently carried out at the Institute of Concrete Structures and Building Materials of the Karlsruhe Institute of Technology are presented in the subsequent chapter. These novel experiments aim to determine the mechanical properties of the corrosion products, which develop under different conditions at the reinforcement. Afterwards, a numerical model is presented, which allows for a realistic evaluation of the stresses and strains inside test specimens that have been produced within the experimental program.

2 EXPERIMENTAL INVESTIGATIONS

2.1 *Cracking mechanism*

The corrosion of reinforcing steel in concrete results in the formation of corrosion products at the surface of the reinforcing bar. The volume of the corrosion products is about 2 to 6 times higher than their initial volume before the formation of rust. The concrete, which surrounds the reinforcement, impedes the increase in volume due to corrosion. This leads to the appearance of an internal pressure within the concrete cover. Its magnitude depends on the corrosion rate. When the internal pressure and the resulting tensile stress, respectively, reaches the tensile strength of the concrete, cracks will appear.

2.2 *Experimental parameters, preparation of specimens*

By means of specific experiments, the time dependent crack development due to reinforcement corrosion is currently monitored and quantified at concrete specimens. The specimens are about 275 concrete cylinders (denoted as corrosion cylinders in the following) with centrically embedded reinforcing bars. The cylindrical shape of the specimens was chosen to establish simple and symmetrical conditions for corrosion and concrete cracking, which allow for a better repeatability during the experiments. Next to different corrosive agents (chloride and carbonation induced corrosion), particularly the influence of material parameters (cement type, w/c-ratio) and geometrical characteristics (diameter of the reinforcing bar, concrete cover thickness) on corrosion are in the focus of the investigations. Table 1 shows the combinations of reinforcing bar diameter d and concrete cover thickness c that were chosen for the fabrication of the different specimens. Either cold-worked plain steel bars (S235JRG2 C+C) were used or reinforcing bars (BSt 500), where the ribs were turned off, except for some validation specimens.

The cylindrical specimens with a height of 30 cm and a diameter D of D = 2c + d (see Fig. 1) were casted upright in cylindrical moulds to avoid accumulation of water at the bottom of the reinforcing bar. The effect of segregation of concrete was minimised by cutting the upper part of the corrosion cylinder after hardening (shortening from 30 to 21 cm). Table 2 provides basic information on the cement type and the concrete composition being used for the preparation of the specimens.

After concreting, the corrosion cylinders remained inside the moulds for three days and were afterwards stored in water until the age of seven days. Subsequently, the specimens were stored in a climate chamber with a standard climate of 20 °C and 65 % RH. These conditions were temporarily interrupted in order to seal the end faces of the cylinders with epoxy resin.

A homogeneously distributed corrosion of the reinforcing bar was realised by means of adding chloride to the fresh concrete or by an accelerated carbonation of concrete (see Tab. 3). Therefore, the specimens were stored in a climate chamber with an increased carbon dioxide content of the surrounding air.

Finally, all specimens were directly exposed to cycles of drying and wetting. For this, the specimens were shortly plunged into water (between 1 and 16 minutes, depending on the concrete cover thick ness) and afterwards stored in standard climate conditions for seven days until the next wetting cycle. This treatment will lead to a uniform corrosion of the reinforcement. Consequently, an axial symmetric loading (two-dimensional) is generally obtained for the specimens, which is a prerequisite for the subsequent numerical analysis.

Table 1. Combination matrix for the geometrical parameters.

Ratio c/d [-]		Concrete cover thickness c [mm]			
		10	20	30	40
Reinforcing bar diameter d [mm]	8	1.3	2.5	–	–
	16	0.6	1.3	–	2.5
	24	0.4	0.8	1.3	1.7

Table 2. Material parameters of the concrete.

Parameter	Name / value
Cement type	OPC (CEM I 32.5 R), BFSC (CEM III/A 32.5 N-NW)
Cement content [kg/m^3]	360
w/c-ratio [-]	0.4, 0.7
Aggregates	sand, gravel
Grading curve	AB 8, BC 8
Chloride content [% by mass of cement]	2.5

Table 3. Corrosion parameters.

Corrosive agent	Concentration	Wet-dry-cycles	w/c-ratio
Chloride	2.5 % by mass of cement	1 to 16 min / 7 d	0.4, 0.7
Carbonation	1.0 % by vol. CO_2	1 to 16 min / 7 d	0.7

Furthermore, laboratory tests were performed to quantify the material properties of the concrete. Among these are tests to identify the compressive and tensile strength as well as the modulus of elasticity and the fracture energy of the concrete. In addition, the shrinkage and creep behaviour of the concrete was determined.

Further investigations using optical microscopy, Raman spectroscopy and computer tomography are currently carried out to identify the type, location and amount of corrosion products that migrate into voids and emerging cracks in the concrete.

2.3 *Strain measurements*

As a consequence of the wetting and drying cycles (see Tab. 3), accelerated corrosion of the reinforcement will lead to early cracking and spalling of the concrete cover at the corrosion cylinders. Upon selected specimens the tangential deformations on the surface of the concrete as well as the chronology and intensity of the internal corrosion pressure are measured. The measurements help to identify and quantify the effects of reinforcement corrosion and allow for the determination of the mechanical properties of the corrosion products.

The measurements are performed on two different kinds of specimens. At first, tangential strains due to corrosion of the centrically embedded reinforcing bars are measured with strain gauges that are glued to the concrete surface along the perimeter of the corrosion cylinders (see Fig. 1). In addition, further measurements take place at modified corrosion cylinders (denoted as hollow cylinders), where the reinforcing bar is replaced by a thin-walled copper tube (wall thickness 0.5 mm) that is filled with hydraulic fluid (see Fig. 2).

As with the regular corrosion cylinders, the tube causes a resistance against shrinkage of the concrete resulting in a residual stress condition inside the specimen. While at the regular corrosion cylinders the internal pressure is caused by the corrosion progress, it is applied hydraulically inside the hollow cylinders. The level of the hydraulic pressure has to be chosen in such a way that the same magnitude of concrete strain is reached at the hollow cylinders as measured and observed at the associated corrosion cylinders simultaneously. The concrete strain is measured by strain gauges being applied in the same way as at the corrosion cylinders. Additionally, strain gauges are attached to the outside surface of the copper tube to measure its tangential strain.

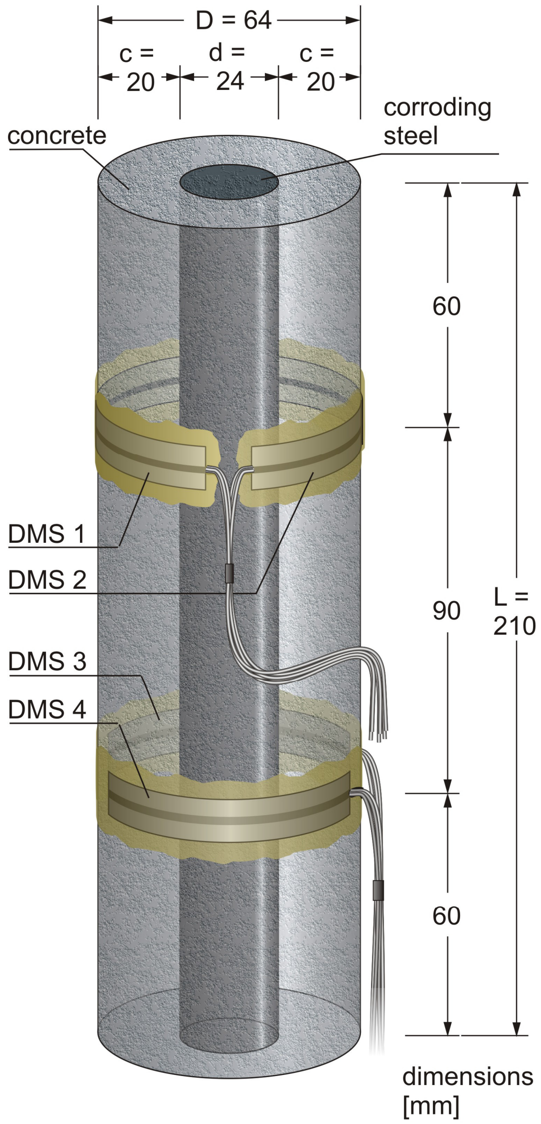

Figure 1. Corrosion cylinder with strain gauges (DMS 1 to 4) to measure tangential strains due to corrosion of the centrically embedded steel bar. The strain gauges are attached with alkali-resistant glue and sealed against moisture ingress.

By means of the assumption, that the hydraulic pressure and the internal pressure due to corrosion cause the same load on the concrete, the time-dependent effects from shrinkage and creep can be eliminated. Thus, the chronology as well as the level of the stresses caused by corrosion can be determined.

Figure 3 shows curves of the moisture and temperature compensated tangential strains which were measured by means of strain gauges that are applied to the concrete surface of each of three corrosion cylinders (see Fig. 1). The concrete strains are caused by carbonation induced corrosion of the steel bar (diameter d = 8/16/24 mm) and were continuously recorded from the start of the wetting and drying cycles (see chapter 2.2) until the occurrence of significant cracks in the concrete cover (cover thickness c = 20 mm, w/c = 0.7, OPC).

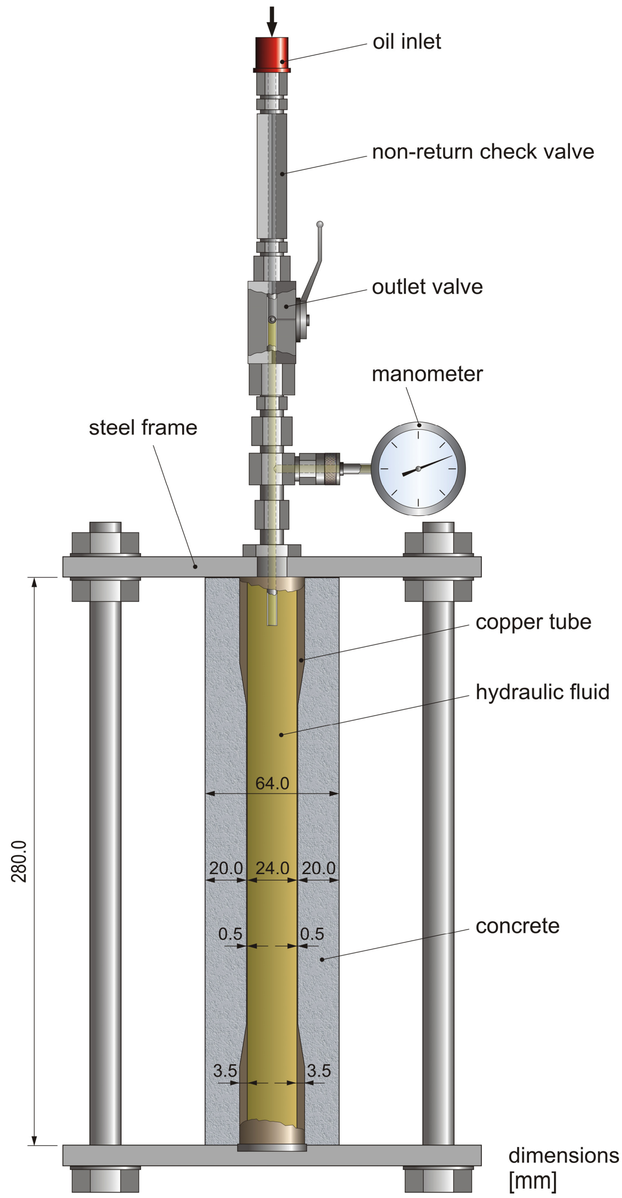

Figure 2. Test facility for application and control of a hydraulic pressure inside a thin-walled copper tube being centrically embedded inside a concrete cylinder. A surrounding steel frame prevents longitudinal deformations.

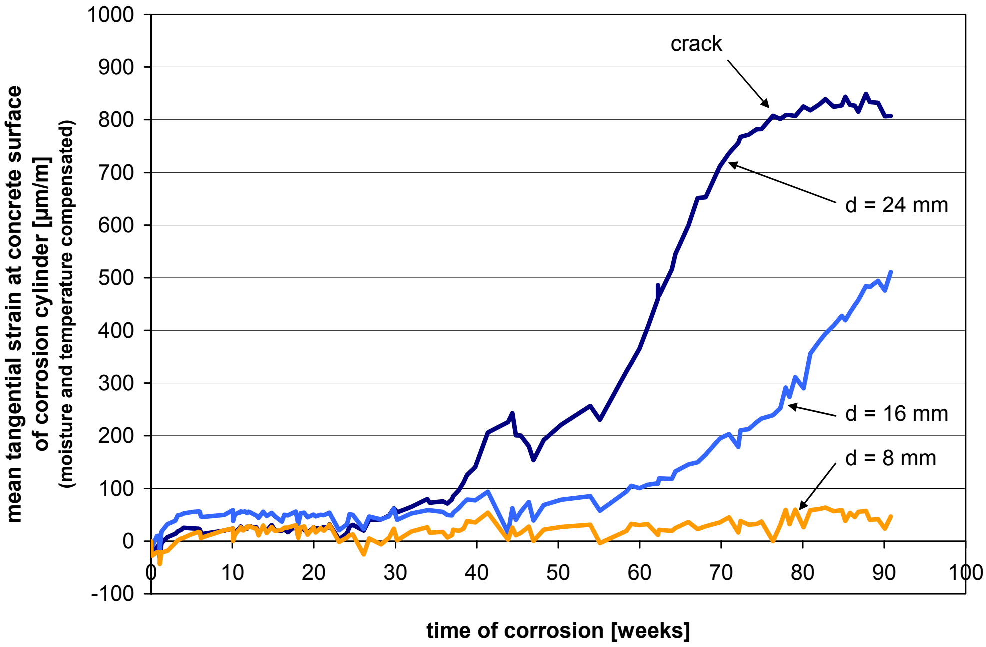

Figure 3. Mean tangential strain at the concrete surface of corrosion cylinders caused by carbonation induced corrosion of the steel bar. The concrete cover thickness c is 20 mm and made of OPC (CEM I 32.5 R) with a w/c-ratio of 0.7. The diameter d of the centrically embedded plain steel bars out of S235JRG2 C+C is 8, 16 and 24 mm.

3 NUMERICAL INVESTIGATIONS

3.1 *Motivation*

The numerical investigations are on the one hand carried out to determine the stresses and strains that can be expected during the experiments. On the other hand, they allow for a detailed analysis of the governing processes during cracking and spalling for different test parameters, and an evaluation of any possible reinforcement configuration of practical relevance. In this paper particularly the influence of the size of the reinforcing bar diameter and the concrete cover are presented.

3.2 *Numerical model*

The numerical simulation is carried out with the finite element software DIANA. The cross section of the specimens, which consists of a centrically in concrete embedded steel bar with a plain surface, is modelled as a two-dimensional finite element mesh (Fig. 4), and allows for analysing plain strain conditions.

The material properties determined in the laboratory tests are implemented in the model. The heterogeneity of the concrete is taken into account by a variance of the tensile strength and fracture energy of each single element. This is considered by defining the appropriate material properties as independent random variables that follow a Gaussian distribution. Further details on this procedure are given in Mechtcherine (2000). For the simulation of crack propagation, the crack band theory according to Bazant & Oh (1983) is used. The tension softening behaviour of the concrete as well as its time dependent behaviour, i.a. creep and shrinkage, are defined according to the CEB-FIP Model Code 1990 (1993).

The corrosion of the reinforcing bar leads to a reduction of the stiffness of the corroding system due to the considerably smaller modulus of elasticity of the corrosion products compared to the original steel. This continuous reduction in stiffness caused

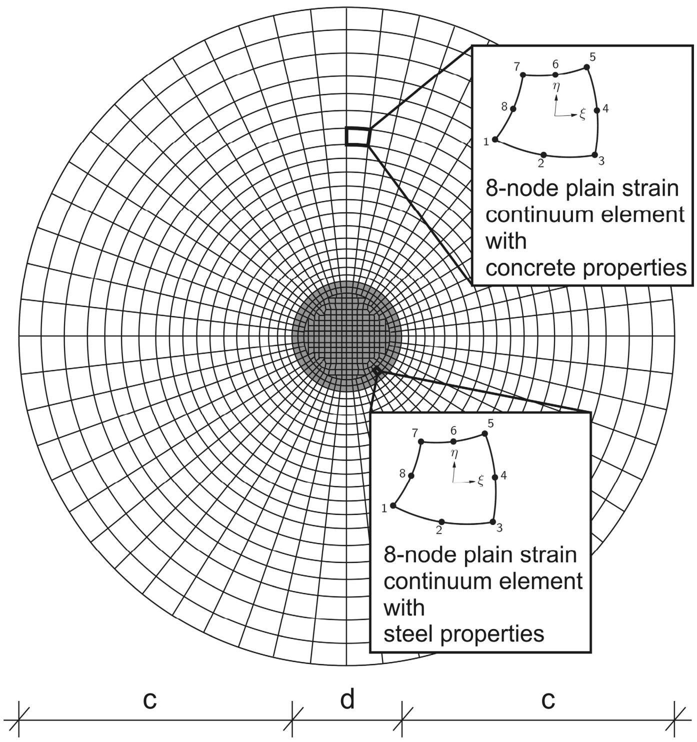

Figure 4. Two-dimensional finite element mesh representing a corrosion cylinder of the model d8c20 (see Tab. 4).

by the increasing growth of corrosion products is also taken into account. The remaining non-corroded steel and the corrosion products are modelled as a composite material in serial order. The reduced stiffness is repeatedly calculated via a user supplied subroutine and imported into the numerical simulation for each time step.

In order to examine the influence of the reinforcing bar diameter and the concrete cover thickness different geometrical variations were modelled and analysed (Tab. 4).

The concrete used in this simulation is characterised by a mean tensile strength f_{ctm} of 1.8 MPa, a mean compressive strength f_{cm} of 21.5 MPa and a modulus of elasticity E of 22000 MPa. The fracture energy G_F of the concrete is assumed to be 0.065 N/mm.

3.3 *Loading function*

The corrosion process and hence the loading that results from the corrosion is a complex procedure, which is governed by the corrosion rate and the volume ratio φ (volume of the rust relative to the volume of the steel). This difference in volume of the corrosion products compared to the original steel takes effect in a rust band that forms on the steel surface (Fig. 5). It can eventually be understood as an increase of the reinforcing bar radius which is constrained by the surrounding concrete and therefore leads to stresses in the concrete cover. By means of the corrosion rate and the volume ratio the free expansion Δr of the reinforcing bar due to uniform corrosion can be assessed by Equation 1. Here, the free expansion is caused by an unhindered adsorption of the total amount of corrosion products on the steel surface (see linear loading function in Fig. 6) which figuratively can be expressed as an increase of the reinforcing bar radius:

$$\Delta r = -\frac{d_i}{2} + \sqrt{\left(\frac{d_i}{2}\right)^2 - \frac{1}{4}\left(d_i^{\,2} - \left(d_i - 2x\right)^2 - \varphi \cdot d_i^{\,2} \cdot \left(1 - \left(1 - \frac{2x}{d_i}\right)^2\right)\right)} \quad (1)$$

where Δr = free increase in reinforcing bar radius [mm]; x = loss of reinforcing bar radius [mm]; d_i = initial reinforcing bar diameter [mm]; φ = volume ratio [-].

It is however possible, that part of the corrosion attack does not lead to stresses in the surrounding concrete as corrosion products migrate into voids around the steel surface (transition zone) or into emerging crack spaces in the concrete.

While in most works the stress development during the filling of voids or cracks is considered to be zero, in the presented work it is assumed that a reduced stress development is taking place during the initial phase of the actual corrosion process. This is justified by the observation that only parts of the corrosion products are able to migrate into the specified spaces without causing stresses while other parts of the corrosion products in fact lead to stresses in the concrete cover in adjacent regions. As well as the measured tangential strains at the surface of the corrosion cylinders at first indicate a minor increase of the developing stress but subsequently show a significant increase of the concrete deformations (see Fig. 3). In the numerical calculations this effect is simply taken into account by an initially reduced but constant gradient of the loading function. This so-called bilinear loading function (see Fig. 6) can be derived with respect to the pore volume in the transition zone. Therefore, at first the loss of reinforcing bar radius x_p has to be determined, which is necessary to fill the voids and pores. The related increase in reinforcing bar radius Δr_p can be calculated using Equation 1. The effective expansion Δr_{corr}, which results from the effective loss of reinforcing bar radius x_{corr} that really leads to stresses in the concrete, can be calculated by subtracting Δr_p from the free increase in reinforcing bar radius Δr.

By analysing the stable crack propagation during the numerical calculations a multilinear loading function that additionally considers the migration of corrosion products into significant cracks can be developed (see Fig. 6).

Table 4. Overview of the analysed finite element models.

Denotation of the model (mesh)	Reinforcing bar diameter d [mm]	Concrete cover c [mm]	Ratio c/d [-]
d8c10	8	10	1.3
d8c20	8	20	2.5
d8c30	8	30	3.8
d16c20	16	20	1.3
d24c20	24	20	0.8
d24c30	24	30	1.3
d24c40	24	40	1.7

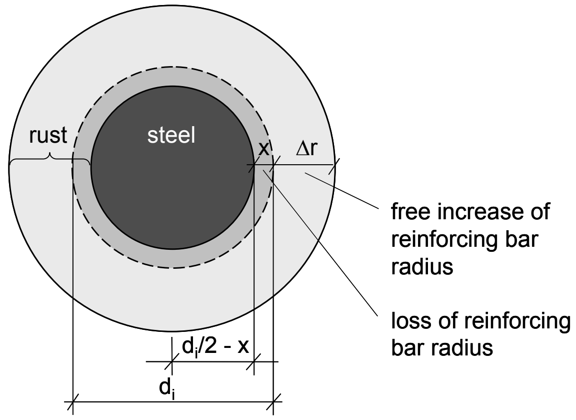

Figure 5. Schematic representation of the free expansion Δr of the reinforcing bar caused by an unhindered adsorption of the total amount of corrosion products on the steel surface due to uniform corrosion which goes along with a loss of reinforcing bar radius x.

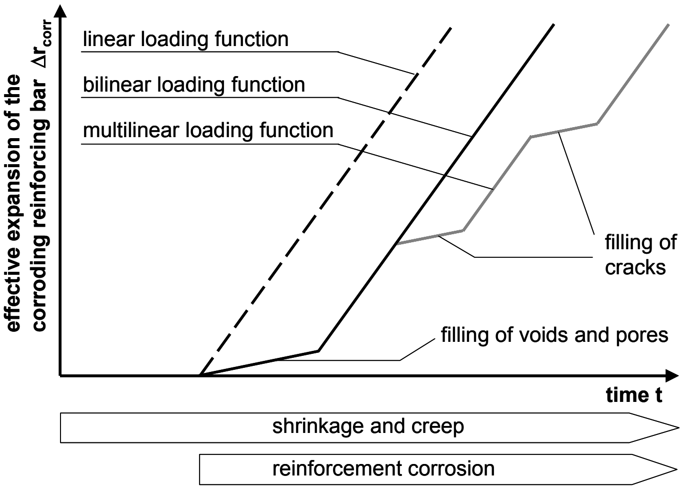

Figure 6. Linear, bilinear and multilinear loading function.

The derivation of the multilinear loading function can be carried out analogous to the procedure chosen for assessing the stress development during the filling of voids and pores.

The effective expansion of the corroding reinforcing bar Δr_{corr} is numerically simulated by a thermal expansion of the steel. This thermal expansion reproduces exactly the respected boundary conditions.

While the above mentioned loading functions are valid for uniform corrosion and thus correspond very well with carbonation induced corrosion, they are not directly suitable for local corrosion effects, so-called pitting corrosion. Pitting corrosion is mostly connected to chloride induced corrosion and usually leads to a very complex three-dimensional stress and strain condition in the concrete. The authors of this paper are aware of the fact, that a three-dimensional problem can only be described inaccurately by means of a two-dimensional model. However, they have decided to develop a two-dimensional model for pitting corrosion since it offers excellent possibilities for studying the corrosion processes and thus leads to a better understanding of corrosion damages.

Val (2007) presented a model to estimate the loss of cross-sectional area of a reinforcing bar due to pitting. It is based on a hemispherical shape of the pit which penetrates the surface of the steel bar and requests knowledge about the pitting factor R (ratio between maximum penetration of pitting and the average penetration depth) and the corrosion rate i_{corr} in terms of a corrosion current density. The maximum depth of a pit can be calculated according to Val (2007) by Equation 2:

$$p(t) = 0.0116 \cdot i_{corr} \cdot t \cdot R \qquad (2)$$

where p = maximum depth of corrosion pit [mm]; i_{corr} = corrosion rate [mm/a]; t = time of corrosion [a]; R = pitting factor [-].

The corrosion penetration can be transformed into an effective local expansion by means of the volume ratio φ and by following the procedure described above. Additionally, the finite element mesh needs to be adapted to allow large local deformations. This can be achieved by a smart implementation of interface elements, as shown in Fig. 7.

Creep and shrinkage of the concrete are taken into account during the entire numerical calculation (all time steps), while the loading resulting from corrosion does not start until a concrete age of eight weeks. This relatively short time was chosen due to numerical reasons, whereas the initiation stage of the corrosion process has not explicitly been considered in this work.

A corrosion rate of 11.5 µm/year, which matches moderate or high corrosion (Broomfield 2007), underlies the simulation results presented in the following chapter. The volume ratio is chosen to be φ = 3.0 for uniform corrosion and φ = 2.0 in case of pitting corrosion respectively.

3.4 *Numerical results*

The calculation of the stresses and strains in the numerical analysis were carried out by time steps. The different loading functions presented in Figure 6 have been applied. In case of uniform corrosion, the stresses in a certain distance from the steel-concrete-interface presented in the Figures 8 and 10 display the mean value of all elements in the same distance from the interface. Figure 8 shows the tangential and radial stresses in the concrete cover for uniform corrosion after 8 weeks (shrinkage only), 26 weeks and 104 weeks for the model d16c20 (denotations see Tab. 4). The stresses in the mainly uncracked specimen (eight weeks) are in good accordance with the analytical solution for a thick-walled hollow cylinder. After significant cracking of the concrete, which takes place after approximately 42 weeks, a stress reduction can be observed.

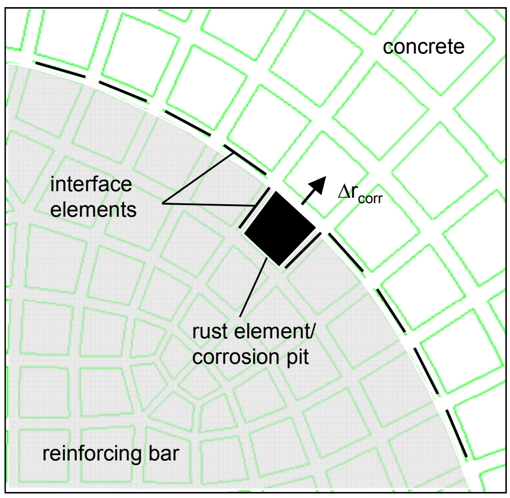

Figure 7. Detail of a two-dimensional finite element mesh of a corrosion cylinder. The local expansion of a rust element representing a corrosion pit is applied by means of implemented interface elements.

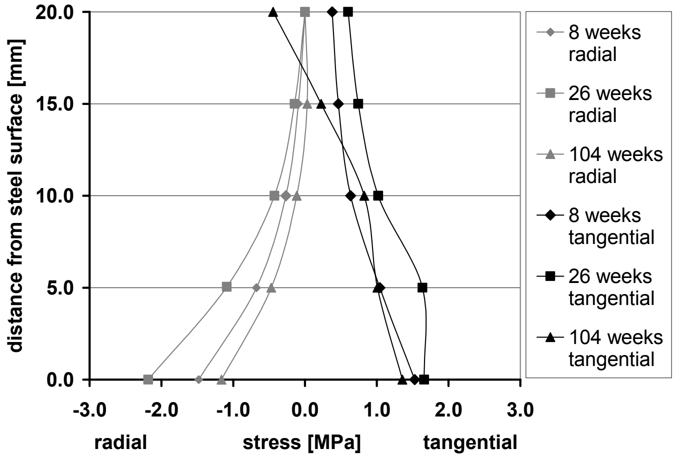

Figure 8. Radial and tangential stresses in the concrete cover due to uniform corrosion after 8, 26 and 104 weeks for the model d16c20 (bilinear loading function).

The steel bar in the centre of the corrosion cylinder constrains the deformations due to shrinkage, which lead to residual stresses that are being reduced by subsequent creep or relaxation, respectively. Already during the first eight weeks these stresses can exceed the tensile strength of the concrete and cause micro-cracking close to the reinforcement (Bohner & Müller 2006). This phenomenon can be observed as well in Fig. 9, left. There are micro-cracks in the transition zone encircling the reinforcing bar. Cracks due to pitting corrosion develop to both sides of the corrosion pit (located at "1h30" at the section of the reinforcing bar) and indicate spalling of the concrete cover. However, after approx. 75 weeks a single crack above the pit dominates and leads to splitting of the concrete cover.

Figure 10 presents the tangential stresses caused by uniform corrosion in the outmost elements for the models d24c20, d24c30 and d24c40 with respect to time. It can be observed that the time until the maximum tensile stress is reached in the concrete surface of the specimens increases with an increasing concrete cover.

The time until cracking of the concrete cover was also analysed by means of the different investigated numerical models (see Tab. 4 and Fig. 11) for both uniform and pitting corrosion. In this context a crack width of about 10^{-5} to 10^{-4} mm corresponds to a cracked element. A general conclusion between the ratio of concrete cover and reinforcing bar diameter (c/d-ratio) and the time to cracking of the concrete cover can not be drawn so far. However as supposed, the time to cracking increases on the one hand with an increasing concrete cover and on the other hand with a decreasing reinforcing bar diameter. The increase in time to cracking caused by a greater concrete cover is considerably more pronounced than the increase due to the decrease in reinforcing bar diameter.

The influence of the loading function has extensively been analysed for the model d16c20. The consideration of the migration of corrosion products into voids in the transition zone (bilinear loading function) leads to an increase of time to cracking of the concrete cover of about 30 % compared to the linear loading function under the assumed conditions for the model d16c20. The prolongation of the time to cracking of the concrete cover depends not only on the volume of the voids in the transition zone, but also on the assumed corrosion rate and volume ratio, as well as the geometrical parameters like concrete cover and reinforcing bar diameter. Consequently, the presented value can not be taken as a general figure.

The additional consideration of the migration of corrosion products into emerging cracks (multilinear loading function) shows only a slight influence compared to the bilinear loading function. The time to cracking of the concrete cover increases to a small extent. It shall be pointed out that for the analysed model D16C20 the c/d-ratio of 1.3 and the concrete cover of 20 mm respectively are not exceptionally large. For specimens with a greater c/d-ratio or a larger concrete cover, which allow for stable crack propagation over a longer period of time, it can be expected that the influence of the multilinear loading function will be more pronounced.

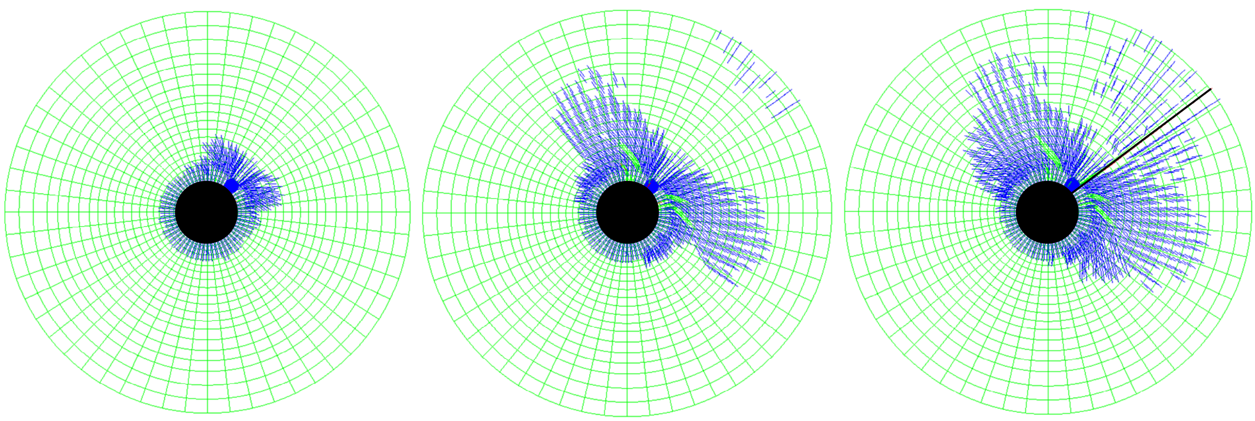

Figure 9. Concrete cover cracking due to pitting corrosion of the reinforcement after 32 (left), 64 (centre) and 75 weeks (right) for the model d8c20 (bilinear loading function).

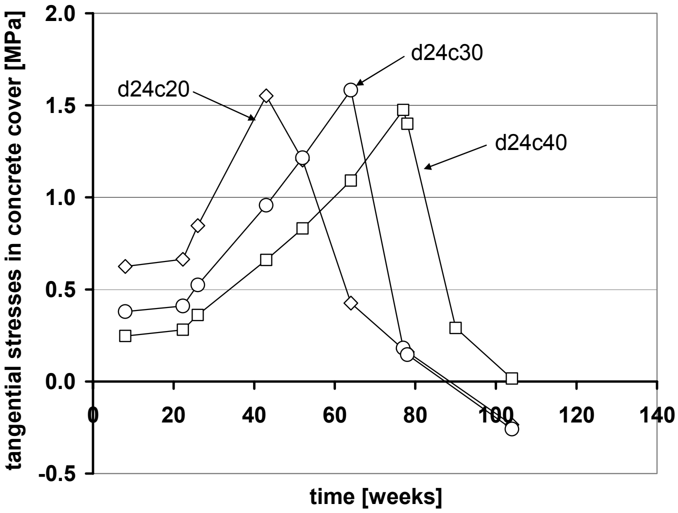

Figure 10. Tangential stresses due to uniform corrosion in the outmost elements with respect to time for the models d24c20, d24c30 and d24c40 (bilinear loading function).

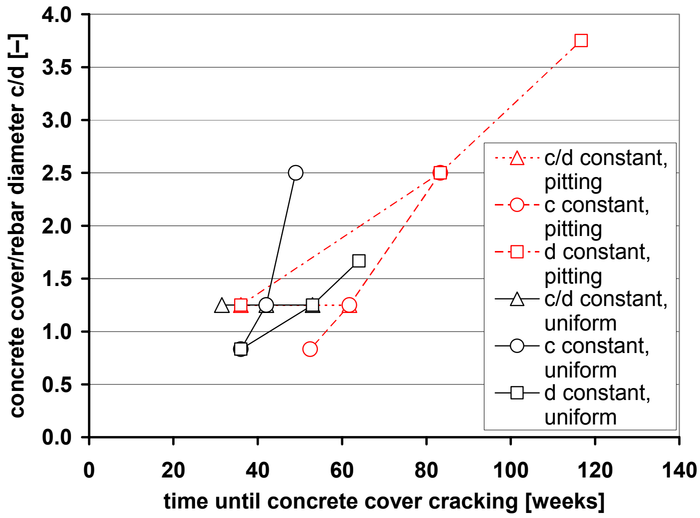

Figure 11. Time to cracking for the outmost elements (crack width 10^{-5} to 10^{-4} mm) investigated on different analysed models (see Tab. 4) for both pitting and uniform corrosion (bilinear loading function).

4 CONCLUSIONS AND OUTLOOK

The presented theoretical and experimental approach allows for estimating the level of stresses and the chronology of appearance of cracks inside the concrete cover, which are caused by the corrosion of the reinforcement. The approach is based on novel experimental investigations being supplemented with numerical analyses.

By means of parameter studies with numerous specimens and on inverse analyses, a prediction model for the time dependent damage process can be derived. The analytic model will be suitable for different and changing conditions regarding the geometry of concrete cover and reinforcing bar diameter, material properties and climatic conditions. It allows for the prediction of the damage development and serves as a part of a complete probabilistic design approach for durability of reinforced concrete structures, which is a future target of the DFG research unit No. 537 of the German Research Foundation (DFG-FOR 537).

ACKNOWLEDGEMENT

The work described in the present paper is part of the DFG research unit No. 537. The financial support from the German Research Foundation is gratefully acknowledged by the authors.

REFERENCES

Bazant, Z.P. & Oh, B.H. 1983. Crack band theory for fracture of concrete. In *Materials and Structures* 16, pp. 155-177

Bhargava, K., Ghosh, A.K., Mori, Y. & Ramanujam, S. 2005. Modeling of time to corrosion-induced cover cracking in reinforced concrete structures. In *Cement and Concrete Research* 35, pp. 2203-2218

Bohner, E. & Müller, H.S. 2006. Modelling of reinforcement corrosion – Investigations on the influence of shrinkage and creep on the development of concrete cracking in the early propagation stage of reinforcement corrosion. In *Materials and Corrosion* 57, No. 12, pp. 940-944

Broomfield, J. 2007. *Corrosion of Steel in Concrete*. London: Taylor & Francis Group, Second Edition

Comité Euro-International du Béton (CEB). 1993. *CEB-FIP Model Code 1990.* Lausanne: CEB Bulletin d'Information, No. 213/214

DFG-FOR 537. German Research Foundation, Research Unit No. 537 (http://for537.cbm.bv.tum.de)

Mechtcherine, V. 2000. Bruchmechanische und fraktologische Untersuchungen zur Rissausbreitung im Beton. In *Schriftenreihe des Instituts für Massivbau und Baustofftechnologie, Universität Karlsruhe*, Heft 40

Toongoenthong, K. & Maekawa, K. 2005. Simulation of coupled corrosive product formation, migration into crack and propagation in reinforced concrete sections. In *Journal of Advanced Concrete Technology* 3, No. 2, pp. 253-265

Val, D.V. 2007. Deterioration of strength of RC beams due to corrosion and its influence on beam reliability. In *Journal of Structural Engineering* 133, No. 9, pp. 1297-1306